

In situ study of calcite-III dimorphism using dynamic diamond anvil cell

Xia Zhao(赵霞), Sheng-Hua Mei(梅升华), Zhi Zheng(郑直), Yue Gao(高悦), Jiang-Zhi Chen(陈姜智), Yue-Gao Liu(刘月高), Jian-Guo Sun(孙建国), Yan Li(李艳), and Jian-Hui Sun(孙建辉)

Citation: Chin. Phys. B, 2022, 31 (**9**): 096201. DOI: 10.1088/1674-1056/ac6157

Journal homepage: http://cpb.iphy.ac.cn; http://iopscience.iop.org/cpb

What follows is a list of articles you may be interested in

High-pressure study of topological semimetals XCd$_2$Sb$_2$ (X = Eu and Yb)

Chuchu Zhu(朱楚楚), Hao Su(苏豪), Erjian Cheng(程二建), Lin Guo(郭琳), Binglin Pan(泮炳霖), Yeyu Huang(黄烨煜), Jiamin Ni(倪佳敏), Yanfeng Guo(郭艳峰), Xiaofan Yang(杨小帆), and Shiyan Li(李世燕)

Chin. Phys. B, 2022, 31 (**7**): 076201. DOI: 10.1088/1674-1056/ac7212

Reaction mechanism of metal and pyrite under high-pressure and high-temperature conditions and improvement of the properties

Yao Wang(王遥), Dan Xu(徐丹), Shan Gao(高姗), Qi Chen(陈启), Dayi Zhou(周大义), Xin Fan(范鑫), Xin-Jian Li(李欣健), Lijie Chang(常立杰),Yuewen Zhang(张跃文), Hongan Ma(马红安), and Xiao-Peng Jia(贾晓鹏)

Chin. Phys. B, 2022, 31 (**6**): 066206. DOI: 10.1088/1674-1056/ac4a72

Bandgap evolution of Mg_3N_2 under pressure: Experimental and theoretical studies

Gang Wu(吴刚), Lu Wang(王璐), Kuo Bao(包括), Xianli Li(李贤丽), Sheng Wang(王升), and Chunhong Xu(徐春红)

Chin. Phys. B, 2022, 31 (**6**): 066205. DOI: 10.1088/1674-1056/ac4cbe

Structural and electrical transport properties of charge density wave material $LaAgSb_2$ under high pressure

Bowen Zhang(张博文), Chao An(安超), Xuliang Chen(陈绪亮), Ying Zhou(周颖), Yonghui Zhou(周永惠), Yifang Yuan(袁亦方), Chunhua Chen(陈春华), Lili Zhang(张丽丽), Xiaoping Yang(杨晓萍), and Zhaorong Yang(杨昭荣)

Chin. Phys. B, 2021, 30 (**7**): 076201. DOI: 10.1088/1674-1056/abf643

Phase transitions in bismuth under rapid compression

Dong-Liang Yang(杨栋亮), Jing Liu(刘景), Chuan-Long Lin(林传龙), Qiu-Min Jing(敬秋民), Yi Zhang(张毅), Yu Gong(宫宇), Yan-Chun Li(李延春), Xiao-Dong Li(李晓东)

Chin. Phys. B, 2019, 28 (**3**): 036201. DOI: 10.1088/1674-1056/28/3/036201

In situ study of calcite-III dimorphism using dynamic diamond anvil cell

Xia Zhao(赵霞)[1,2], Sheng-Hua Mei(梅升华)[1,†], Zhi Zheng(郑直)[1], Yue Gao(高悦)[1,2], Jiang-Zhi Chen(陈姜智)[1], Yue-Gao Liu(刘月高)[1], Jian-Guo Sun(孙建国)[3], Yan Li(李艳)[1,2], and Jian-Hui Sun(孙建辉)[1]

[1] *CAS Key Laboratory for Experimental Study under Deep-sea Extreme Conditions, Institute of Deep-sea Science and Engineering, Chinese Academy of Sciences (CAS), Sanya* 572000, *China*

[2] *University of Chinese Academy of Sciences, Beijing* 100049, *China*

[3] *Department of Mechanical Engineering, National University of Singapore (NUS), Singapore* 117575, *Singapore*

(Received 9 December 2021; revised manuscript received 21 March 2022; accepted manuscript online 28 March 2022)

The phase transitions among the high-pressure polymorphic forms of $CaCO_3$ (cc-I, cc-II, cc-III, and cc-IIIb) are investigated by dynamic diamond anvil cell (dDAC) and *in situ* Raman spectroscopy. Experiments are carried out at room temperature and high pressures up to 12.8 GPa with the pressurizing rate varying from 0.006 GPa/s to 0.056 GPa/s. *In situ* observation shows that with the increase of pressure, calcite transforms from cc-I to cc-II at $\sim$ 1.5 GPa and from cc-II to cc-III at $\sim$ 2.5 GPa, and transitions are independent of the pressurizing rate. Further, as the pressure continues to increase, the cc-IIIb begins to appear and coexists with cc-III within a pressure range that is inversely proportional to the pressurizing rate. At the pressurizing rates of 0.006, 0.012, 0.021, and 0.056 GPa/s, the coexistence pressure ranges of cc-III and cc-IIIb are 2.8 GPa–9.8 GPa, 3.1 GPa–6.9 GPa, 2.7 GPa–6.0 GPa, and 2.8 GPa–4.5 GPa, respectively. The dependence of the coexistence on the pressurizing rate may result from the influence of pressurizing rate on the activation process of transition by reducing the energy barrier. The higher the pressurizing rate, the lower the energy barrier is, and the easier it is to pull the system out of the coexistence state. The results of this *in situ* study provide new insights into the understanding of the phase transition of calcite.

Keywords: calcite-III, dimorphism, dynamic diamond anvil cell, *in situ* Raman spectroscopy, pressurizing rate

PACS: 62.50.–p, 33.20.Fb, 47.80.Fg, 91.65.–n **DOI:** 10.1088/1674-1056/ac6157

1. Introduction

As the main carbon carriers, carbonate minerals control the migration of carbon in different geochemical reservoirs.[1–4] Calcite ($CaCO_3$), the most common carbonate mineral, has over 12 proven structural polymorphs, such as calcite-I–calcite-VII (cc-I–cc-VII), aragonite, and pyroxene $CaCO_3$.[2,5–12] Although it is accepted that calcite reacts with enstatite in the upper mantle to form dolomite,[13] the diamond inclusions and ancient subduction zone rocks suggest that calcite could exist at the top of the lower mantle.[14–16] Under the mantle pressure and temperature condition, calcite must undergo a substantial phase transition to adapt the changes in pressure and temperature with the depth.[2,5,6,11,17,18] Owing to its pressure sensitivity, structural phase transitions in calcite may also be used as geobarometers.[19] Thus, phase transition in calcite is of great importance in understanding the structure and dynamics of the Earth.

The pressure-induced phase transition of cc-III dimorphism at room temperature has been extensively studied.[2,20–24] Despite a long history of investigation, the transition process among the dimorphisms of calcite, cc-III in triclinic and cc-IIIb in pseudomonoclinic triclinic structure, remains unclear. On the one hand, some researchers claimed that the cc-III and cc-IIIb can coexist in the same pressure range. For example, Liu and Mernagh identified the coexistence of cc-III and cc-IIIb at a pressure of 5.2 GPa, based on the observation of different cell parameters and Raman vibrational modes.[20] The coexistence was later confirmed by Merlini *et al*. but at a lower pressure of 3 GPa in polycrystalline samples.[21] Yuan *et al*. further determined the coexisting pressure range to be 1.97 GPa–3.38 GPa.[25] On the other hand, several researchers observed that each phase exists separately in different pressure ranges. For example, Pippinger *et al*. found that the pressure ranges for the existence of cc-IIIb and cc-III are 2.14 GPa–3.14 GPa and 3.42 GPa–5.42 GPa, respectively, at a temperature of 298 K, and the pressure ranges change to 2.2 GPa–3.71 GPa and 3.84 GPa–4.45 GPa, respectively, at a temperature of 283 K.[22] In both cases, the cc-IIIb and cc-III do not coexist. Furthermore, there are also studies suggesting that cc-IIIb may appear or disappear repeatedly with the increase of pressure, which complicates the issue even more. Koch–Mueller *et al*. found experimentally that the cc-IIIb first appears at 2.2 GPa, then disappears at $\sim$ 3 GPa due to the transition to cc-III, and finally reappears at $\sim$ 5 GPa.[24] The first-principle simulation also indicated that the transition between cc-IIIb and cc-III can oscillate as pressure increases from cc-IIIb to cc-III at 4.3 GPa and then from cc-III to cc-IIIb at 14.9 GPa.[23] These findings are summarized in Fig. 1.

[†]Corresponding author. E-mail: mei@idsse.ac.cn

© 2022 Chinese Physical Society and IOP Publishing Ltd

In order to clarify the coexistence of cc-III and cc-IIIb, it is necessary to conduct further research.

In addition, the Earth's interior is persistently in the process of dynamic evolution, including seafloor spreading and plate subduction.[26–29] Some geological zones, such as those around fault zones during earthquakes or adjacent areas during volcanic eruptions, may be squeezed at a high pressurizing rate. Accordingly, the physical and chemical properties of the constituent minerals including calcite in the relevant Earth interior should be affected by these dynamic processes. For example, different carbonates (dolomite, aragonite, calcite, magnesite) were found in different high-pressure (HP) metamorphic rocks (metapelite, marble, eclogite) from the Western Tianshan subduction zone.[30] Rapid magma ascents contacted calcite inclusions within quartz phenocrysts at Santa Rita, New Mexico (USA).[31] However, up to now, the studies aiming at exploring the physical and chemical processes in the Earth's interior, whether mineral physics or mineral chemistry, were mainly carried out under static conditions, and the dynamic research is almost blank. Undoubtedly, it is of great scientific significance to carry out dynamic research of the high-pressure phase transition of calcite under the conditions of temperature and pressure simulating mineral occurrence environment in geological processes.

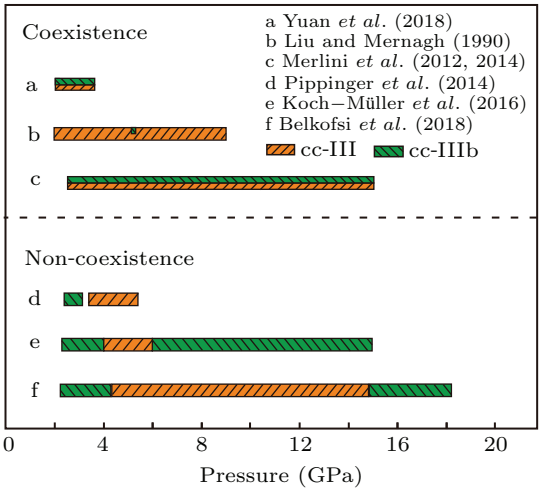


Fig. 1. Summary of previous results of coexistence of cc-III and cc-IIIb at room temperature. Merlini *et al.* (2012) found that both cc-III and cc-IIIb can be stable in a pressure range of 2.5 GPa–15 GPa.[2] Later (2014), they observed the coexistence of these two phases at a pressure of $\sim$ 3 GPa.[21]

The spectral analysis provides useful information about the phase transitions in solids. Specifically, Raman scattering occurs when monochromatic light interacts with molecular vibrations inside a crystal. With the spectrum being able to record any change in bonding structure, Raman spectroscopy is used extensively in the study of phase transition in calcite.[5,7,20,32–40] The isolated carbonate ion $[CO_3]^{2-}$ has four distinct vibration bands: symmetric stretching mode (ν_1), out-of-plane bending mode (ν_2), asymmetric stretching mode (ν_3), and in-plane bending mode (ν_4). Carbonate minerals also have two lattice vibration bands reflecting the lattice vibration (translation and oscillation) between Ca^{2+} and $[CO_3]^{2-}$.[41] The Raman spectra of rhombohedral cc-I are characterized by five Raman-active peaks located at 156, 282, 712 ($= \nu_4$), 1085 ($= \nu_1$), and 1434 cm^{-1} ($= \nu_3$), respectively.[37] Owing to the high sensitivity in pressure, the change of ν_4 mode often receives special attention in the spectral analysis of phase changes in calcite. In calcite, the cc-I and cc-II have different crystal structures: the former is rhombohedral ($R3c$) and the latter is monoclinic ($P2_1/m$). The transition from cc-I to cc-II is achieved by shifting Ca^{2+} cations and rotating the $[CO_3]^{2-}$ group $\sim 11°$.[25,42] Correspondingly, the ν_4 mode in the Raman spectrum will split from one peak for cc-I into two peaks for cc-II. The structure of cc-III is less symmetrical than that of cc-II. The change from cc-II to cc-III results from the breaking of the triclinic (P) symmetry within the thermodynamically stable field of cc-III.[2] This change reflected in the Raman spectra is that the ν_4 mode changes from two to more than five peaks, which has been confirmed by Pippinger *et al.*[22] and Yuan *et al.*[25]

Diamond anvil cell (DAC) has been used extensively in high-pressure studies due to its capability of being incorporated with spectrum analysis techniques, and the understanding of the calcite phase has been greatly improved with the DAC technique.[6–10,43] However, the observation of detailed structure change is a challenge to the conventional DAC technique. In the conventional DAC, the increase of pressure in the experiment can only be achieved step-by-step mechanically. Because of a large pressure interval produced by discontinuous pressurizing, some transient processes, such as the coexistence of phases, could be easily overlooked. Dynamic loading DAC (dDAC) was developed from the conventional DAC. At a designated rate, it can provide continuous pressurizing. Several dDAC studies[44–48] on mineral phases (including Raman studies on carbon tetrachloride and ice, and x-ray diffraction studies on KCl and zirconium) have demonstrated the prospect of this new technology.

In this study, using the dDAC combined with Raman spectral analysis, we realize *in situ* monitoring of calcite phase transition upon pressure increasing. Our results confirm the coexistence of cc-III and cc-IIIb, and the pressure range of the coexistence depends on the pressurizing rate. More importantly, our discovery reveals that kinetics plays a key role in controlling the transition, which may provide an insight into the structural transition in calcite.

2. Materials and methods

2.1. Sample composition

All samples for DAC experiments in this study were from the same natural calcite crystal (see Fig. S1). The crystal was

colorless and transparent, about 3 cm in diameter. Scanning electron microscopy (SEM) image and x-ray energy dispersive spectrum (EDS) of the crystal were taken on a Phenom ProX microscope (see Fig. S2). The EDS results confirmed the high purity of $CaCO_3$ crystal containing only three major elements: calcium, carbon, and oxygen.

2.2. Experimental procedure

High-pressure experiments of the single-crystal calcite were performed at the CAS Key Laboratory for Experimental Study under Deep-sea Extreme Conditions, Institute of Deep-sea Science and Engineering, Chinese Academy of Sciences (Sanya, Hainan, China). Experiments were carried out on our dDAC system, which combines piezoelectric actuators and conventional DAC. Conventional DAC was located between pillars and pressure screws (see Fig. S3). The sample assembly was the same as that in a conventional DAC, equipped with two type-IIA low-fluorescence diamonds with 300-μm culets. The sample chamber was a hole of ∼ 100 μm in diameter, produced by a Drilex-2000 laser punch, located in the center of a stainless-steel gasket of 100 μm in thickness. Water was used as a pressure-transmitting medium. In the process of sample assembly, a ruby particle was enclosed with the sample in the sample chamber as a pressure indicator, and the pressure was measured by *in situ* ruby fluorescence.[49]

The dDAC device provides controllable loading functions. By setting the target pressure and loading path (*i.e.*, the times for loading–stay–unloading) in advance through the signal generator, selected loading modes including the designated loading rate could be obtained. The correctness of the input signal was ensured by an oscilloscope (see Fig. S4).

Combined with spectral analysis technology, our high-pressure test system has the capability of *in situ* observation. The Raman and fluorescence spectra of calcite and ruby were simultaneously collected by a charge coupled device (CCD) detector and an intensified CCD (ICCD) detector, respectively. The Raman spectra from 100 cm^{-1} to 930 cm^{-1} were recorded by an Andor Shamrock SR500i spectrometer equipped with a Leica DM2700 microscope, and a Plan Apo SL Infinity Corrected 20× objective with a numerical aperture value of 0.28. The excitation laser was a 532-nm frequency-doubled Nd:YAG laser. A 1800-gr·mm^{-1} holographic grating coupled with a CCD detector (2000×256 pixels per inch, 1 inch = 2.54 cm) with a spectral resolution of 1.5 cm^{-1} was used for the Raman spectrum measurement. Raman spectra of calcite at room temperature and atmospheric pressure were recorded to ensure a good instrument condition, and three standard Raman-active peaks were located at 156, 282, and 712 cm^{-1} (= ν_4), respectively. A 600-gr·mm^{-1} holographic grating coupled with an ICCD detector (1024×1024 pixels per inch) was used to measure the ruby fluorescence spectra. The exposure time for fluorescence and Raman spectra were about 1 s and 4 s, respectively. The time-resolved Raman spectrogram in the dynamic loading process is shown in Fig. 2.

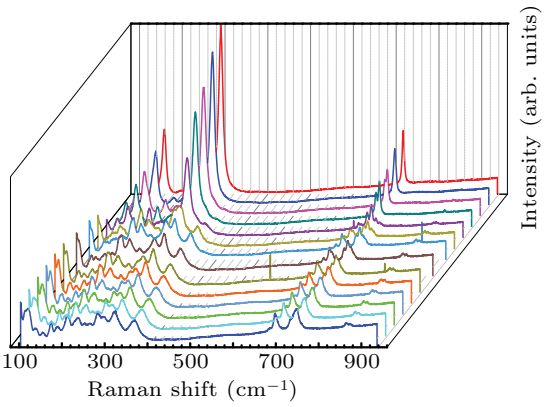


Fig. 2. Typical time-resolved Raman spectra for calcite investigated in dynamic loading process.

2.3. *Ab initio* simulation using density functional theory

To corroborate the experimental Raman spectra, we used Materials Studio to calculate the Raman peaks of cc-III and cc-IIIb. The basic setup was similar to that in Bayarjargal *et al.*[39] with an 880-eV plane-wave cut-off and Monkhorst–Pack grids[50] of 1×1×1 grid parameters. We also used the same criterion of self-consistency as that in Bayarjargal *et al.*,[39] and the maximum displacement is 0.005 Å.

3. Results and discussion

3.1. Experimental conditions

Eight experiments from five samples (C1, C2, C3, C4, and C5) are performed with dDAC. Experiments are carried out at high pressures and different pressurizing rates. The detailed information for all runs is summarized in Table 1.

Table 1. Pressure and loading rate settings for experiments.

Sample No.	Run No.	Initial pressure P_i (GPa)	Pressurizing rate dP/dt (GPa/s)	Peak pressure P_{peak} (GPa)
C1	DD0005	0.5	0.056	10.4
C2	DD0006	1.3	0.012	8.4
C3	DD0012	0.6	0.013	5.1
	DD0013	4.5	0.012	8.6
C4	DD0015	1.6	0.006	6.7
	DD0016	4.9	0.004	9.2
	DD0017	6.8	0.007	12.8
C5	DD0110	0.8	0.021	6.1

3.2. Raman spectrum analyses

Previous studies revealed that in calcite, the phase transition leads the characteristic mode ν_4 to split (*e.g.*, from one peak for cc-I to two peaks for cc-II, to more than five peaks for cc-III); the feature is therefore used to identify the phase state in calcite. While there is consensus on the feature of ν_4 mode of cc-I, cc-II, and cc-III, the feature of ν_4 for cc-IIIb remains uncertain. In this case, we try to find clues through *ab*

initio simulation to reveal the relationship between the bonding structure and the feature of their characteristic mode ν_4 for both cc-III and cc-IIIb.

We perform first-principle simulations based on DFT for the characteristic ν_4 mode of $CaCO_3$ at a spectra resolution of 4 cm^{-1} separately at a pressure of 2.2 GPa and 7 GPa. As presented in Fig. 3, cc-III shows seven peaks at 2.2 GPa and eight peaks at 7 GPa, while cc-IIIb exhibits three peaks at both pressures. Therefore, we use the features of ν_4 mode: three peaks for cc-IIIb and more than seven for cc-III, as the criterion to identify cc-IIIb and cc-III in our analysis. The simulation results are in good agreement with previous observations. For example, Yuan *et al*. observed that the ν_4 mode in calcite shows 3 sharp peaks in cc-IIIb, and splits into 5 peaks in cc-III.[25] Similarly, Pippinger *et al*. found that the ν_4 mode in calcite changes from 4 to 7 peaks in the process of phase transition from cc-IIIb into cc-III.[22]

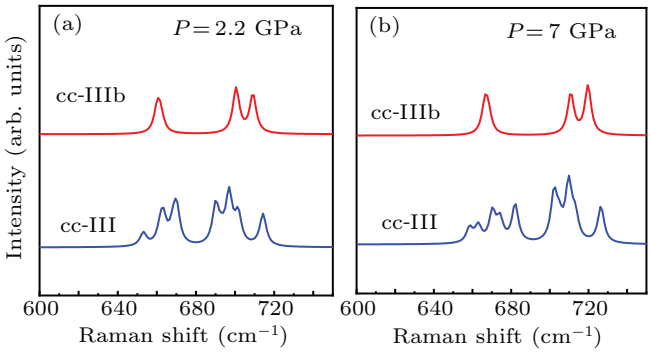


Fig. 3. Curves of characteristic ν_4 mode of calcite, by first-principle simulation, for cc-III and cc-IIIb at $P = 2.2$ GPa (a) and 7 GPa (b).

3.3. Transition from cc-I to cc-II and from cc-II to cc-III

Although this study focuses on the dimorphism of cc-III, the transition from cc-I to cc-II and from cc-II to cc-III, which are essential steps for the introduction of cc-III, need to be analyzed systematically.

Figure 4 shows the Raman spectra recorded from run DD0012, indicating the transition of calcite from cc-I to cc-II. When the pressure rises to about 1.8 GPa, the vibration mode of ν_4 splits into two peaks (713.5 cm^{-1} and 718.8 cm^{-1}) from one (715.5 cm^{-1}), which indicates the occurrence of the phase transition from cc-I to cc-II. The same phenomenon is observed in other runs, but the transition pressure is slightly different.

The transition of calcite from cc-II to cc-III can be observed in the Raman spectra collected from run DD0006 as shown in Fig. 5. In the phase of cc-II, the doublet ν_4 peaks are located respectively at 712.3 cm^{-1} and 721.3 cm^{-1} at 2.2 GPa. When the pressure reaches 2.7 GPa, the doublet ν_4 mode splits into eight peaks, located at 679.3, 693.1, 698.3, 712.9, 723.7, 733.0, 741.8, and 748.2 cm^{-1}, respectively. This indicates the transition from cc-II to cc-III, and there is a transient process before the completion of phase transition, in which cc-II coexists with cc-III (*e.g.*, at $P \approx 2.4$ GPa). Experimental results regarding the transitions, from cc-I to cc-II and from cc-II to cc-III, obtained from all runs are summarized in Table 2.

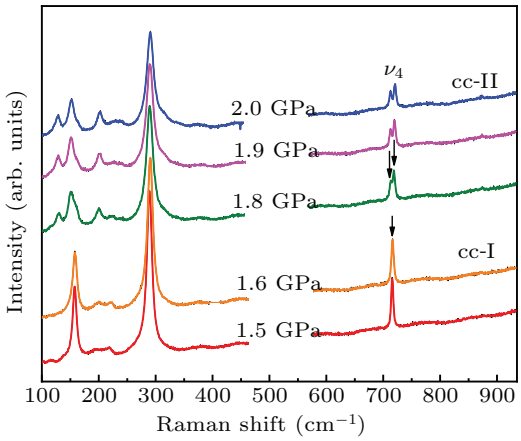


Fig. 4. Raman spectra recorded from run DD0012 under dynamic loading pressurizing. At $P \approx 1.8$ GPa, the vibration mode of ν_4 splits from one peak to two peaks, indicating the transition of calcite from cc-I into cc-II.

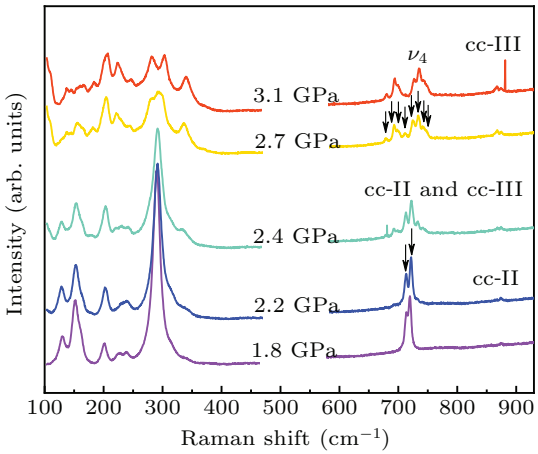


Fig. 5. Raman spectra collected from run DD0006 under dynamic loading pressurizing. The vibration mode of ν_4 splits from two peaks at $P \approx 2.2$ GPa to eight peaks at 2.7 GPa, indicating the transition of calcite from cc-II to cc-III. There is a transient process before the completion of phase transition at ~ 2.4 GPa, in which cc-II coexists with cc-III.

Table 2. Pressure conditions (P, in unit of GPa) for the stability of each phase and coexistence of cc-III dimorphism in calcite.

Round No.	cc-I	cc-II	cc-III	cc-III and cc-IIIb	cc-IIIb
DD0005				2.8–4.5	4.5-
DD0006	0–1.7	1.8–2.2	2.7–3.1	3.3–6.4	6.7-
DD0012–13	0–1.6	1.8–1.9	2.2–2.6	3.1–6.9	7.0-
DD0015–17	0–1.7	1.7–2.1	2.2–2.7	2.8–9.8	9.9-
DD0110	0–1.3	1.4–1.7	2.3	2.7–6.0	6.1-

Our results show that the transition pressures from cc-I to cc-II and from cc-II to cc-III are around 1.5 ± 0.3 GPa and 2.5 ± 0.3 GPa, respectively. Although the transition pressure from cc-I to cc-II is consistent with most of previous studies,[5,24,42,51,52] the transition pressure from cc-II to cc-III agrees only with some of the results[20,25] at a pressure of about 2.5 GPa. We attribute the discrepancy between this

study and others in the transition pressure from cc-II to cc-III to the ambiguity of the cc-III and cc-IIIb dimorphisms. In some researches, cc-II is preferentially transformed into cc-IIIb rather than cc-III as pressure increases.[22–24] As a result, the transition pressure from cc-II to cc-III cannot be compared with their results, because the transition did not occur in their studies.

3.4. Coexistence of cc-III and cc-IIIb

As mentioned above, the dimorphism of cc-III is the focus of this study, and more attention is paid to the coexistence of cc-III and cc-IIIb. These two phases, based on the analyses of their vibrational characteristics, can be recognized from their ν_4 mode, with seven or more peaks for cc-III and three for cc-IIIb. Figure 6 shows the Raman spectra in the pressure range for the coexistence of cc-III and cc-IIIb. At $P \approx 3.1$ GPa, the characteristic ν_4 mode exhibits eight peaks, located respectively at 679.3, 693.1, 699.5, 711.2, 724.5, 733.8, 742.2, and 747.9 cm^{-1}, indicating that the calcite is in cc-III phase. As the pressure increases, the ν_4 mode changes continuously. At $P \approx 3.3$ GPa, the peak located at 710.8 cm^{-1} disappears, indicating the beginning of the phase transition from cc-III into cc-IIIb. At 6.7 GPa, the ν_4 mode shows mainly three peaks at 699.1, 745.0, and 750.7 cm^{-1}, marking the completion of the phase transition from cc-III to cc-IIIb. From that point on, a few weak external modes appear or disappear with pressure increasing, but the ν_4 mode remains almost unchanged,

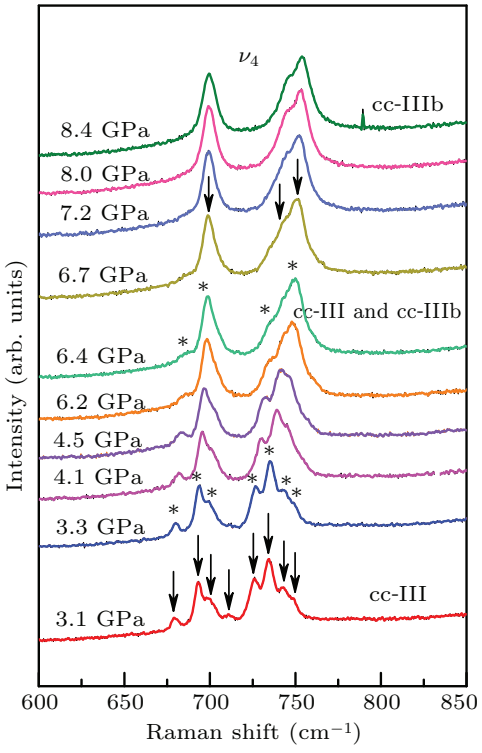


Fig. 6. Raman spectra recorded from run DD0006 under dynamic-loading pressurizing. The ν_4 mode changes from eight peaks at 3.1 GPa into three peaks at 6.7 GPa, indicating the phase transition of calcite from cc-III to cc-IIIb. Between these two pressures, two phases coexist.

indicating that calcite is stable in cc-IIIb phase. In the pressure range between 3.3 GPa and 6.4 GPa, however, the peaks representing cc-III diminish and the feature for cc-IIIb emerges, which can be considered as the coexistent pressure range of cc-III and cc-IIIb. Similar results are obtained in all other runs, which are summarized in Table 2.

Through continuously pressurizing and *in situ* spectroscopic observations, we confirm the coexistence of cc-III and cc-IIIb. Although the coexistent pressure range varies slightly run by run, our observations are consistent with previous studies in which coexistence was also found.[2,20,21,25]

3.5. Influence of pressurizing rates on phase transition

In order to evaluate the influence of pressurizing rate on the phase transition of calcite, experiments are carried out at different pressurizing rates. The effect of pressurizing rate on the phase transition of calcite is displayed in Fig. 7.

As shown in Fig. 7, at different pressurizing rates, the transition pressures from cc-I to cc-II and from cc-II to cc-III are ~ 1.5 GPa and ~ 2.5 GPa, respectively, indicating that the transition pressures are not influenced by the pressurizing rate. In comparison, the transition pressures from cc-III to cc-IIIb are ~ 9.9, ~ 6.9, ~ 6.1, and ~ 4.5 GPa for the pressurizing rate of 0.006, 0.012, 0.021, and 0.056 GPa/s, respectively. The transition pressure decreases with the increase of pressurizing rate, showing a remarkable pressurizing rate dependence.

Furthermore, it is found that the pressure range for the coexistence of cc-III and cc-IIIb is also dependent on the pressurizing rate. As shown in Fig. 7, as the pressurizing rate increases from 0.006 GPa/s to 0.056 GPa/s, the pressure range for the coexistence of cc-III and cc-IIIb decreases from ~ 7 GPa to ~ 1.5 GPa. The higher the pressurizing rate, the narrower the coexistence pressure range of cc-III to cc-IIIb is.

Our results show that part of the phase transition process of calcite is related to the pressurizing rate, while the other part is independent of the pressurizing rate. This phenomenon can be explained from the perspective of energy.

In thermodynamics, a system tends to be in an energy "well" (that is, the Gibbs energy is the lowest) to remain stable. In order to adapt to the changes of thermodynamic conditions (such as pressure), the system must find new energy well accordingly. Although thermodynamics provides the driving force to bring the system from one well to another, effective activation energy ($Q_{\rm eff}$) is required to overcome an energy barrier (Q) for completing the transition. In other studies,[53] it is found that the $Q_{\rm eff}$ decreases exponentially with the pressurizing rate. The points mentioned here are schematically illustrated in Fig. S5 for later discussion.

Comparing with the transition of calcite from cc-I to cc-II, and cc-III, the coexistence of cc-III and cc-IIIb can be regarded as a metastable state with a lower energy barrier for the next transition. If the transition between the two states

with a high Q, even if the Q is reduced to $Q_{\rm eff}$ due to the influence of pressurizing rate, the reduced part of the energy, $\Delta Q = Q - Q_{\rm eff} \ll Q$, is still too small to affect considerably the transition process. So, the effect of the pressurization rate is not obvious. However, for the metastable state of the coexistence of cc-III and cc-IIIb with a low Q, any change of ΔQ resulting from the influence of pressurizing rate (say, $\Delta Q \sim Q$ can be significant. The higher the pressurizing rate, the lower the energy barrier is, and the easier it is to pull the system out of the metastable state. This is very consistent with our observations shown in Fig. 7.

Our results suggest that the coexistence of cc-III and cc-IIIb depends on the pressurizing rate and may provide clues to the explaining of the lack of observed coexistence in some static studies. In the conventional DAC, each stage of step-by-step pressurization is commonly completed in a very short time, that is, the pressurizing rate is very high. As shown in Fig. 7, the higher the pressurizing rate, the narrower the coexistence pressure range is. Since the pressurizing rate in stepwise-loading DAC can be several orders of magnitude higher than the fastest pressurizing rate in this study, it is not surprising that the coexistence, if any, of cc-III and cc-IIIb is overlooked in those researches carried out by the conventional DAC.

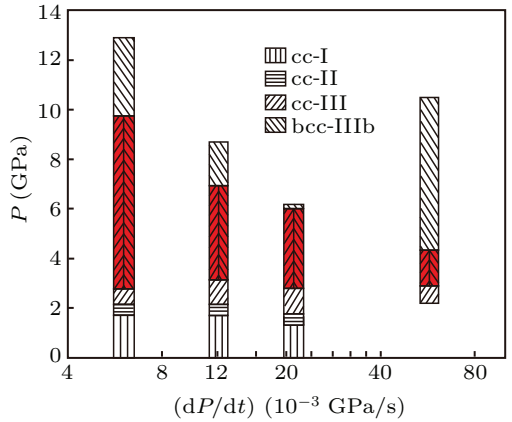


Fig. 7. Variations of transition pressures on calcite phase with the pressurizing rate for cc-I, cc-II, cc-III, and cc-IIIb. The portion of the coexistence of cc-III and cc-IIIb are highlighted and the pressurizing rate is log-scaled.

4. Conclusions

Using the d-DAC, the phase transitions in calcite, from cc-I to cc-II, cc-III, and cc-IIIb, are investigated based on *in situ* experiments. A number of new findings are revealed, especially about the coexistence of cc-III dimorphism, which are summarized as follows.

(i) At room temperature, the phase transitions of $CaCO_3$ from cc-I to cc-II and from cc-II to cc-III occur at $\sim$ 1.5 GPa and $\sim$ 2.5 GPa, respectively. The pressures of these transitions are independent of the pressurizing rate.

(ii) The transition pressure from cc-III to cc-IIIb is pressurizing rate dependent. As the pressurizing rate increases from 0.006 GPa/s to 0.056 GPa/s, the transition pressure decreases from 9.8 GPa to 4.5 GPa.

(iii) The transition from cc-III to cc-IIIb is a sluggish process. Before the complete transition from cc-III to cc-IIIb, those two phases can coexist in a certain pressure range, which is dependent on the pressurizing rate. The higher the pressurizing rate, the narrower the pressure range for the coexistence of the two phases is.

(iv) The dependence of the coexistence of cc-III to cc-IIIb on pressurizing rate may result from the influence of pressurizing rate on the activation process by reducing energy barrier. The higher the pressurizing rate, the lower the energy barrier is, and the easier it is to pull the system out of the metastable state.

This study marks some of the first attempts of *in situ* Raman spectroscopy of mineral phase transition in dynamic loading DAC. It reveals that the phase transition of solid can be pressure-rate-dependent, providing new insights into the understanding of the structural changes of minerals in the dynamic environment.

Acknowledgements

We are indebted to Junwei Li for his technical help in the experiment. We want to thank High Performance Computing (HPC), NUS for providing technical support in part of our simulation work.

Project supported by the Fund from the Chinese Academy of Sciences (Grant No. QYZDY-SSW-DQC029) and the National Natural Science Foundation of China (Grant No. 41674097).

References

[1] Dasgupta R and Hirschmann M M 2010 *Earth and Planetary Science Letters* **298** 1
[2] Merlini M, Hanfland M and Crichton W A 2012 *Earth and Planetary Science Letters* **333** 265
[3] Liu Y, Li W, Lu X, Liu Y, Ruan B and Liu X 2017 *Ore Geology Reviews* **91** 419
[4] Zhang Z W, Wang Y L, Qian B, Liu Y G, Zhang D Y, Lu P R and Dong J 2018 *Ore Geology Reviews* **96** 236
[5] Suito K, Namba J, Horikawa T, Taniguchi Y, Sakurai N, Kobayashi M, Onodera A, Shimomura O and Kikegawa T 2001 *American Mineralogist* **86** 997
[6] Hagiya K, Matsui M, Kimura Y and Akahama Y 2005 *Journal of Mineralogical and Petrological Sciences* **100** 31
[7] Catalli K and Williams Q 2005 *American Mineralogist* **90** 1679
[8] Ono S, Kikegawa T and Ohishi Y 2007 *American Mineralogist* **92** 1246
[9] Oganov A R, Glass C W and Ono S 2006 *Earth and Planetary Science Letters* **241** 95
[10] Oganov A R, Ono S, Ma Y, Glass C W and Garcia A 2008 *Earth and Planetary Science Letters* **273** 38
[11] Gavryushkin P N, Martirosyan N S, Inerbaev T M, Popov Z I, Rashchenko S V, Likhacheva A Y, Lobanov S S, Goncharov A F, Prakapenka V B and Litasov K D 2017 *Crystal Growth and Design* **17** 6291
[12] Li X, Zhang Z, Lin J F, Ni H, Prakapenka V B and Mao Z 2018 *Geophysical Research Letters* **45** 1355
[13] Kushiro I 1975 *Earth and Planetary Science Letters* **28** 116
[14] Ague J J and Nicolescu S 2014 *Nature Geoscience* **7** 355

[15] Kaminsky F, Matzel J, Jacobsen B, Hutcheon I and Wirth R 2016 *Mineralogy and Petrology* **110** 379
[16] Wirth R, Kaminsky F, Matsyuk S and Schreiber A 2009 *Earth and Planetary Science Letters* **286** 292
[17] Nestola F, Korolev N, Kopylova M, Rotiroti N, Pearson D G, Pamato M G, Alvaro M, Peruzzo L, Gurney J J, Moore A E and Davidson J 2018 *Nature* **555** 237
[18] Hou M, Zhang Q, Tao R, Liu H, Kono Y, Mao H K, Yang W, Chen B and Fei Y 2019 *Nat. Commun.* **10** 1963
[19] Hacker B R, Kirby S H and Bohlen S R 1992 *Science* **258** 110
[20] Liu L G and Mernagh T P 1990 *American Mineralogist* **75** 801
[21] Merlini M, Crichton W A, Chantel J, Guignard J and Poli S 2014 *Mineralogical Magazine* **78** 225
[22] Pippinger T, Miletich R, Merlini M, Lotti P, Schouwink P, Yagi T, Crichton W A and Hanfland M 2014 *Physics and Chemistry of Minerals* **42** 29
[23] Belkofsi R, Adjaoud O and Belabbas I 2018 *Modelling and Simulation in Materials Science and Engineering* **26** 065004
[24] Koch-Mueller M, Jahn S, Birkholz N, Ritter E and Schade U 2016 *Physics and Chemistry of Minerals* **43** 545
[25] Yuan X, Gao C and Gao J 2019 *Mineralogical Magazine* **83** 191
[26] Beaussier S J, Gerya T V and Burg J P 2019 *Tectonophysics* **763** 1
[27] Hynes A 1987 *Precambrian Research* **36** 189
[28] Choe H and Dyment J 2021 *Eaeth and Planetary Science Letters* **561** 116787
[29] Choe H and Dyment J 2020 *Geophysical Research Letters* **47** e2019GL085975
[30] Tao R, Zhang L and Zhang L 2020 *Geoscience Frontiers* **11** 915
[31] Audetat A, Pettke T and Dolejs D 2004 *Lithos* **72** 147
[32] Katz S and Schock R N 1968 *American Mineralogist* **53** 1910
[33] Cifrulak S D 1970 *American Mineralogist* **55** 815
[34] Fong M Y and Nicol M 1971 *J. Chem. Phys.* **54** 579
[35] Adams D M and Pogson M 1988 *Spectrochimica Acta Part A: Molecular Spectroscopy* **44** 745
[36] Williams Q, Collerson B and Knittle E 1992 *American Mineralogist* **77** 1158
[37] Gillet P, Biellmann C, Reynard B and McMillan P 1993 *Physics and Chemistry of Minerals* **20** 1
[38] Wang S and Zheng H 2011 *Spectroscopy and Spectral Analysis* **31** 2117
[39] Bayarjargal L, Fruhner C J, Schrodt N and Winkler B 2018 *Physics of the Earth and Planetary Interiors* **281** 31
[40] Fu W and Yuan X 2019 *Spectroscope and Spectral Analysis* **39** 2053 (in Chinese)
[41] Bischoff W D, Sharma S K and Mackenzie F T 1985 *American Mineralogist* **70** 581
[42] Merrill L and Bassett W A 1975 *Acta Crystallographica Section B: Structural Crystallography and Crystal Chemistry* **31** 343
[43] Ono S, Kikegawa T, Ohishi Y and Tsuchiya J 2005 *American Mineralogist* **90** 667
[44] Yuan C, Zhang X, Zhou L, Li H, Feng S, Yang K and Zhu X 2021 *Journal of Molecular Liquids* **328** 115444
[45] Lin C, Smith J S, Sinogeikin S V, Park C, Kono Y, Kenney-Benson C, Rod E and Shen G 2016 *J. Appl. Phys.* **119** 045902
[46] Chen J Y, Kim M, Yoo C S, Liermann H P and Evans W 2014 *J. Phys.: Conf. Ser.* **500** 142006
[47] Velisavljevic N, Sinogeikin S, Saavedra R, Chellappa R S, Rothkirch A, Dattelbaum D M, Konopkova Z, Liermann H P, Bishop M, Tsoi G M and Vohra Y K 2014 *J. Phys.: Conf. Ser.* **500** 032020
[48] Chen J Y and Yoo C S 2011 *Proc. Natl. Acad. Sci. USA* **108** 7685
[49] Mao H K and Bell P M 1978 *Science* **200** 1145
[50] Monkhorst H J and Pack J D 1976 *Phys. Rev. B* **13** 5188
[51] Jamieson J C 1957 *Journal of Geology* **65** 334
[52] Bridgman P W 1939 *American Journal of Science* **237** 7
[53] Lin C and Tse J S 2021 *J. Phys. Chem. Lett.* **12** 8024